Recoil energy distributions for dissociation of the van der Waals molecule *p*-difluorobenzene–Ar with 450–3000 cm^{-1} excess energy

Susan M. Bellm and Warren D. Lawrance[a)]
School of Chemistry, Physics and Earth Sciences, Flinders University, G.P.O. Box 2100, Adelaide, SA 5001, Australia

(Received 23 November 2004; accepted 20 December 2004; published online 8 March 2005)

Velocity map imaging has been used to measure the distributions of translational energy released in the dissociation of *p*-difluorobenzene–Ar van der Waals complexes from the $\overline{5^1}$, $\overline{3^1}$, $\overline{5^2}$, $\overline{3^1 5^1}$, $\overline{5^3}$, $\overline{3^2}$, and $\overline{3^2 5^1}$ states. These states span 818–3317 cm^{-1} of vibrational energy and correspond to a range of energies above dissociation of 451–2950 cm^{-1}. The translational energy release (recoil energy) distributions are remarkably similar, peaking at very low energy (10–20 cm^{-1}) and decaying in an exponential fashion to approach zero near 300 cm^{-1}. The average translational energy released is small, shows no dependence on the initial vibrational energy, and spans the range 58–72 cm^{-1} for the vibrational levels probed. The average value for the seven levels studied is 63 cm^{-1}. The low fraction of transfer to translation is qualitatively in accord with Ewing's momentum gap model [G. E. Ewing, Faraday Discuss. **73**, 325 (1982)]. No evidence is found in the distributions for a high energy tail, although it is likely that the experiment is not sufficiently sensitive to detect a low fraction of transfer at high translational energies. The average translational energy released is lower than has been seen in comparable systems dissociating from triplet and cation states. © *2005 American Institute of Physics*. [DOI: 10.1063/1.1858434]

I. INTRODUCTION

Although the translational energy released in the dissociation of benzene dimers was reported more than 20 years ago,[1] there is only a handful of experimental studies of the translational energy released in van der Waals molecule dissociation. Recently, Yoder *et al.* reported the first use of the velocity map imaging (VMI) technique for this purpose, measuring the kinetic energy released during dissociation of pyrazine–Ar complexes from the triplet state.[2] Yoder and Barker subsequently used a time-of-flight method to measure the kinetic energy released in the dissociation of 18 aromatic–*X* complexes (where *X* is a monatomic, diatomic, or small polyatomic) from the triplet state.[3] Our group has used velocity map imaging to determine the binding energy of a number of van der Waals molecules[4–6] and to determine distributions for the translational energy released for several molecular systems including benzene–$(Ar)_n^+$ $(n=1,2)$,[7] *p*-difluorobenzene–Ar (*p*DFB–Ar) neutral and cation species,[8] and benzene–Ar.[9] A feature of all studies is that only a small fraction of the excess energy is released as kinetic energy. The remainder must be partitioned into rotation and vibration of the fragments. Our study of the dissociation of *p*DFB–Ar from the $\overline{5^1}$ level in S_1 and $\underline{29_2}$ level in D_0 $(p\text{DFB–Ar})^+$ showed that where there are few vibrational levels available in the polyatomic fragment, rotational excitation is the most significant energy reservoir.[8] The same conclusion was reached for dissociation of benzene–Ar from $\overline{6^1}$.[9] Other studies have also shown significant rotational excitation in the fragments, suggesting that this is not unusual in the sparse region of the vibrational manifold of the aromatic product.[10–14]

Yoder and Barker's study produced triplet species by intersystem crossing from the 0° level of the van der Waals complex in S_1.[3] The T_1 energies ranged from ~2500 to 8600 cm^{-1}. Complexes involving different aromatic moities had quite different initial T_1 vibrational energies, but all were in a region of medium to high vibrational state density. The translational energy release (TER) distributions are reasonably similar for a given complexed atom or molecule, leading the authors to conclude that the average recoil energy is not strongly influenced by the initial vibrational energy or density of states of the donor. Table I shows the average translational energy released for the aromatic–Ar complexes studied by Yoder and Barker.

These authors followed their experimental study with

TABLE I. The aromatic–Ar complexes studied by Yoder and Barker, their initial triplet energies, and the average translational energy released (Ref. 3).

Complex	Initial vibrational energy (cm^{-1})	Average recoil energy (cm^{-1})[a]
Pyrimidine–Ar	2543	130
Pyrazine–Ar	4056	100, 111
Methylpyrazine–Ar	~4056	157
Aniline–Ar	7236	196, 243
Benzene–Ar	~8600	163
Toluene–Ar	~8600	185

[a]The values listed have been calculated from the distribution parameters reported by Yoder and Barker (Ref. 3). They are somewhat larger than the values given in Ref. 3. The authors have reexamined their data and concur with the values reported here (Ref. 57).

[a)]Author to whom correspondence should be addressed. Fax: 61-8-8201 2905. Electronic mail: warren.lawrance@flinders.edu.au

quasiclassical trajectory calculations of the dissociation of pyrazine–Ar and methylpyrazine–Ar complexes.[15] The calculations showed little variation with initial vibrational energy, consistent with the experimental observations, although the lowest vibrational excitation studied was 4000 cm^{-1} where the density of vibrational destination states is already quite high. Translational energy release distributions were found to be similar for van der Waals molecule dissociation and collision-induced transfer at temperatures below 300 K. Interestingly, the rotational energy distributions for the aromatic fragment were found to be similar to the translational energy release distributions, with matching average values.

Yoder and Barker's work[3,15] suggests that, at least when the density of product vibrational states is high, the translational energy released is not strongly dependent on the initial vibrational energy or state density. Interestingly, their calculations predict that for aromatic-atom complexes the rotational energy distribution of the aromatic product is essentially the same as the total translational energy distribution. Our experiments on *p*DFB–Ar (Ref. 8) and benzene–Ar (Ref. 9) at low initial vibrational energy show significantly higher rotational excitation of the *p*DFB product than translational energy released, contrary to the situation computed for higher energy complexes. There is a gap in our knowledge of how the product vibrational, rotational, and translational distributions evolve as the destination vibrations progress from a sparse to high density regime. While various studies have examined the vibrational energy distribution within the aromatic product,[8–14,16–26] there has been no systematic study of the evolution in the translational or rotational product state distributions with increasing vibrational energy within the complex.

Here we report a study of the translational energy released during dissociation of *p*DFB–Ar complexes from seven vibrational levels with energies spanning the range 818–3317 cm^{-1}. This corresponds to a range of energies above dissociation of 451–2950 cm^{-1}. Our study complements that of Yoder and Barker who, as we have noted, studied transfer from a range of complexes at higher initial energies. By studying dissociation of a single complex, we examine how the translational energy distributions evolve as the available energy and density of destination vibrations increase substantially.

This study allows us to also explore the related issue of collision-induced energy transfer. Previous studies of the dissociation dynamics have shown that dissociation is occurring far from the equilibrium geometry.[8,9] The barriers calculated for movement of the Ar atom show that it can move from the plane above the ring to below it prior to dissociation.[27–29] This suggests that the complex can dissociate from a large range of geometries and is less constrained than is suggested by the initial geometry.

*p*DFB–Ar was chosen as it has been studied extensively. The $S_1 \leftarrow S_0$ spectroscopy of the *p*DFB chromophore is well known.[30,31] Dispersed fluorescence and mass analyzed threshold ionisation (MATI) experiments have established the vibrational distributions within the *p*DFB product following dissociation from the lower lying vibrations (<1000 cm^{-1}).[11,20–23] VMI has been used to determine the binding energy in the S_0 and S_1 states of the neutral and D_0 state of the cation.[4,5]

II. EXPERIMENTAL DETAILS AND DATA ANALYSIS

The experimental setup and the method of data analysis have been described in detail in a previous publication from this group.[7] Briefly, the experiment operates as follows. A 1% mixture of *p*DFB in argon at a stagnation pressure of $\sim$300 kPa is introduced into the main chamber as a pulsed supersonic expansion. After passing through a skimmer the expansion enters the ionization region of a Wiley–McLaren time-of-flight mass spectrometer. A frequency doubled dye laser intersects the expansion in the centre of the first acceleration region. The UV beam is collimated to $\sim$2–3 mm diameter in the interaction region and operated at low power (on the order of microjoules). This is done to ensure that only a few ions are produced each laser shot, thereby eliminating the possibility of coulombic repulsion contributing to the fragment velocities. The dye laser excites complexes to an S_1 vibrational level. Dissociation from that level produces S_1 *p*DFB products that are ionized by absorption of a second photon. Ions are accelerated in two stages, travel through a field-free region, and strike a position sensitive detector (dual microchannel plate/phosphor screen combination). The electrode potentials are adjusted so that the instrument operates in velocity map imaging mode.[32] The detector is gated on to coincide with the arrival time of $p\text{DFB}^+$ ions. The phosphor screen image is captured by a charge-coupled device (CCD) camera and downloaded to a computer that determines the center positions of the ions detected. These are stored as a histogram of ion count versus position on the detector.[33,34] The process continues until an image is obtained with the desired signal to noise ratio.

For each transition investigated images were obtained with the dye laser wavelength tuned to the maximum of the transition. For the S_1 levels studied, dissociation of the complex is rapid and occurs predominantly on the S_1 surface, as discussed in Sec. III. A background image, off-resonance from the transition, was obtained over the same number of laser shots as the signal image. The background signal is due to residual *p*DFB in the chamber that is not removed between gas pulses.

The three-dimensional distribution can be recreated from the two-dimensional image using an inverse Abel transform.[35] Since all images show an isotropic distribution, indicating that dissociation occurs on a time scale slower than molecular rotation, consistent with previous measurements,[22,36] the two-dimensional distribution can be collapsed to a one-dimensional distribution of intensity versus image radius (a so-called radial plot). Radial plots were generated for each image. The background radial plot was subtracted from the signal radial plot to give the true signal radial plot. Because the absorption by residual *p*DFB changes slightly with wavelength, some scaling of the background was necessary. This is done to match the "signal" and background values at very high radius where the true signal is zero. The resulting distributions were processed using the

TABLE II. The vibrational levels from which we have monitored the translational energy released in dissociation of *p*DFB–Ar complexes. The initial vibrational energy of the complex and the energy available to the fragments is shown.

Initial level	S_1 vibrational energy (cm^{-1})	Available energy (cm^{-1})
$\overline{5^1}$	818	449
$\overline{3^1}$	1251	882
$\overline{5^2}$	1633	1264
$\overline{3^1 5^1}$	2068	1699
$\overline{3^2}$	2500	2131
$\overline{5^3}$	2447	2078
$\overline{3^2 5^1}$	3317	2948

second inverse Abel transform method described in Ref. 37. The energy scale was calibrated using photoelectron images of *p*DFB. Previously published zero kinetic energy (ZEKE) photoelectron spectra of *p*DFB (Ref. 38) are used to calibrate the photoelectron images, and this calibration is then applied to the van der Waals dissociation images. The total kinetic energy released to the fragments is calculated from conservation of momentum. The intensity in the transformed distribution is corrected to provide the desired distribution of intensity versus total translational energy released as discussed in Ref. 2.

The translational energy distributions are fitted with functions of the form:

$$F(E) = \sqrt{E}\sum_{i=1}^{n} A_i \exp(-k_i E), \tag{1}$$

which is the form that arises when the radial plot is expressed as a sum of n Gaussian functions. Having $n=2$ was sufficient to obtain a good fit to the distributions. Functions of this form have previously been used to describe the translational energy probability distribution of dissociating van der Waals clusters.[7]

The low translational energy region of the distributions is masked by signal from uncomplexed *p*DFB which appears as a sharp spike at the center of all the images. For this reason the low energy region (ca. $0-10$ cm^{-1}) is ignored in the analysis procedure.

III. RESULTS

We have measured the translational energy distributions after exciting seven vibrational levels within the S_1 state: $\overline{5^1}$, $\overline{3^1}$, $\overline{5^2}$, $\overline{3^1 5^1}$, $\overline{5^3}$, $\overline{3^2}$, and $\overline{3^2 5^1}$. The assignment of the $\overline{5^1_0}$, $\overline{3^1_0}$, $\overline{5^2_0}$, $\overline{3^1_0 5^1_0}$, $\overline{3^2_0}$, $\overline{5^3_0}$, and $\overline{3^2_0 5^1_0}$ transitions is based on the *p*DFB spectral assignments reported by Knight and Kable[30] and the known *p*DFB–Ar redshift of 30 cm^{-1}.[20,21] The *p*DFB–Ar transitions were confirmed using velocity and mass resolved resonantly enhanced multiphoton ionization (VMR-REMPI) as discussed in Ref. 39. The excess energy of each of these levels above the S_1 dissociation threshold (D^1_0) is shown in Table II. This excess energy is distributed amongst the translational, rotational, and vibrational degrees of freedom of the products. Since one product is an atom, all rotation and vibration is in the *p*DFB fragment.

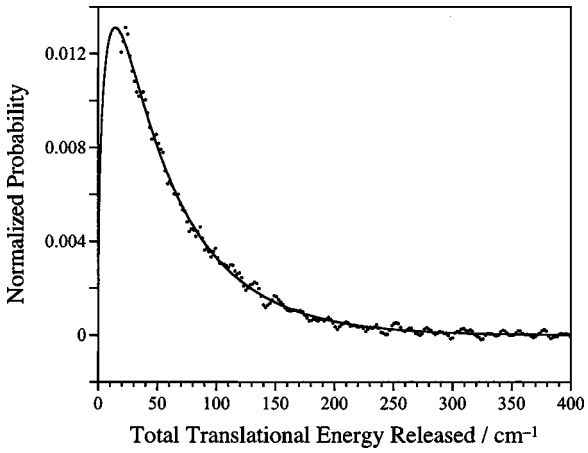

FIG. 1. Translational energy release distribution for *p*DFB–Ar dissociation from the $\overline{3^1}$ ($E_{vib}=1251$ cm^{-1}) level. This distribution is illustrative of the high signal level distributions. The solid line is a fit using Eq. (1) with $n=2$.

Since we are comparing the TER distributions for dissociation from each of these levels to determine the vibrational energy dependence of the distributions, it is important to establish that dissociation occurs in the S_1 state of the neutral rather than the ground electronic state of the ion following $1+1$ REMPI of the complex. For dissociation to occur in S_1, it must be rapid to ensure that it occurs before the complex absorbs a second photon.

We have established previously that $74\% \pm 9\%$ of *p*DFB–Ar molecules excited via $\overline{5^1_0}$ dissociate in S_1.[8] Jacobson, Humphrey, and Rice have measured the rate of vibrational predissociation (VP) from a number of S_1 levels for the *p*DFB–Ar complex.[36] For $\overline{5^1}$ they report a VP lifetime, τ_{VP}, of 4.3 ± 0.5 ns. Thus levels with $\tau_{VP} < 4.3$ ns will have in excess of 75% of dissociation occurring in S_1. Of the other levels studied here VP lifetimes are reported for $\overline{3^1}$ and $\overline{5^2}$. For $\overline{3^1}$ VP was too fast to measure accurately and $\tau_{VP} < 1.5$ ns. For $\overline{5^2}$ $\tau_{VP}=3.7$ ns, slightly faster than observed for $\overline{5^1}$.

VP rates have not been reported for the states above $\overline{5^2}$, i.e., $\overline{3^1 5^1}$, $\overline{3^2}$, $\overline{5^3}$ and $\overline{3^2 5^1}$. However, the rate of dissociation will increase for these states as a consequence of the onset of rapid intramolecular vibrational redistribution (IVR) within the *p*DFB molecule. At lower vibrational energies the vibrational predissociation dynamics of *p*DFB–Ar are nonstatistical because dissociation of van der Waals clusters is hindered by inefficient coupling between high frequency molecular vibrational modes and low frequency intermolecular van der Waals modes.[20–23,26] The onset of rapid IVR within *p*DFB results in the transfer of energy to low frequency vibrational modes in *p*DFB,[40,41] which couple more efficiently with the low frequency van der Waals modes. Hence dissociation will occur rapidly in S_1 at energies above the onset of IVR within the *p*DFB moiety. Zhang, Smith, and Knee observed IVR from $3^1 5^1$ (2068 cm^{-1}) and higher levels in their molecular beam study.[42] Restricted IVR was observed for the bands in the $2000-2500$ cm^{-1} region, with recurrences in the time behavior. The addition of van der Waals modes in the complex will increase the density of states significantly and is thereby expected to lead to irre-

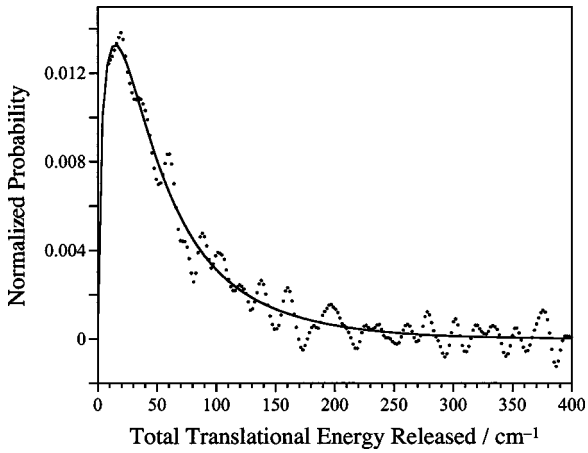

FIG. 2. Translational energy release distribution for *p*DFB–Ar dissociation from the $\overline{3^2}$ (E_{vib}=2500 cm^{-1}) level. This distribution is illustrative of the lowest signal levels obtained. The solid line is a fit using Eq. (1) with n=2.

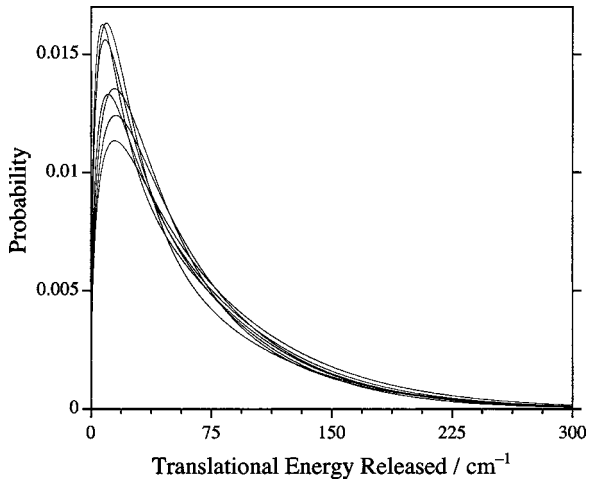

FIG. 3. A plot of the fits to the TER distributions for all levels studied. The distribution has been plotted on a linear scale, which accents the differences at low translational energy. Figure 4 shows the data plotted on a logarithmic scale. The distributions from the seven levels are remarkably similar.

versible IVR by providing a route for vibrational energy to leak from the states accessed in the initial IVR step. For this reason we believe that irreversible IVR will occur rapidly within *p*DFB–Ar for $\overline{3^1 5^1}$ and higher lying levels. We conclude that for all levels studied dissociation is sufficiently rapid in S_1 for the distributions to pertain to that state.

TER distributions for *p*DFB–Ar dissociation from $\overline{3^1}$ (E_{vib}=1251 cm^{-1}) and $\overline{3^2}$ (E_{vib}=2500 cm^{-1}) are shown in Figs. 1 and 2, respectively. They show the extremes of the signal-to-noise level. The solid lines are fits to the distribution by a function of the form of Eq. (1) involving two terms. The parameters for all distributions are summarized in Table III. Figures 3 and 4 show the fits to the TER distributions for all levels studied. These have been plotted linearly in Fig. 3, which accentuates the differences at low translational energy, and logarithmically in Fig. 4, which enhances the differences at high energy. Figures 3 and 4 show that the distributions from the seven levels are remarkably similar, peaking at very low energies (~10–20 cm^{-1}) and decaying in an exponential-like fashion, approaching zero around 300 cm^{-1}.

IV. DISCUSSION

A. Average translational energy released

The experimental results, revealed by examination of Figs. 3 and 4, show that the recoil energy does not change significantly with increasing internal energy of the initially excited level over the range 818–3317 cm^{-1}. It is remarkable that the distribution is so little changed whether there are only a handful of destination vibrations available or many hundred. The translational energy released to the fragments is only a small fraction of the excess energy. This is quantified in Table IV, which shows the average translational energy released for dissociation from each of the initial states. These data are plotted in Fig. 5. It can be seen that the values span a narrow range. The average value is 63 cm^{-1}. At the highest level studied, $\overline{3^2 5^1}$ (E_{vib}=3317 cm^{-1}), the excess energy is almost 3000 cm^{-1} yet the average translational energy released is only 65 cm^{-1}. The amount of energy partitioned into translation is essentially constant with increasing initial energy of the complex, so the fraction of the available energy appearing in translation is decreasing. The remaining energy is partitioned between vibration and rotation of the *p*DFB product. A small amount of energy in translation of the product is expected given Yoder and Barker's observations for dissociation from triplet levels with E_{vib}~2600–8600 cm^{-1}.

TABLE III. A_i and k_i values for the fits [Eq. (1)] to the experimental recoil energy distributions for *p*DFB–Ar.

Transition	A_1	k_1	A_2	k_2
$\overline{5_0^1}$	0.007 17	0.0646	0.001 68	0.0181
$\overline{3_0^1}$	0.003 61	0.0478	0.002 19	0.0199
$\overline{5_0^2}$	0.007 79	0.0993	0.002 61	0.0206
$\overline{3_0^1 5_0^1}$	0.002 77	0.0216	0.006 24	0.0841
$\overline{5_0^3}$	0.002 17	0.0180	0.002 86	0.0540
$\overline{3_0^2}$	0.004 40	0.0409	0.001 27	0.0174
$\overline{3_0^2 5_0^1}$	0.004 57	0.0722	0.002 41	0.0194

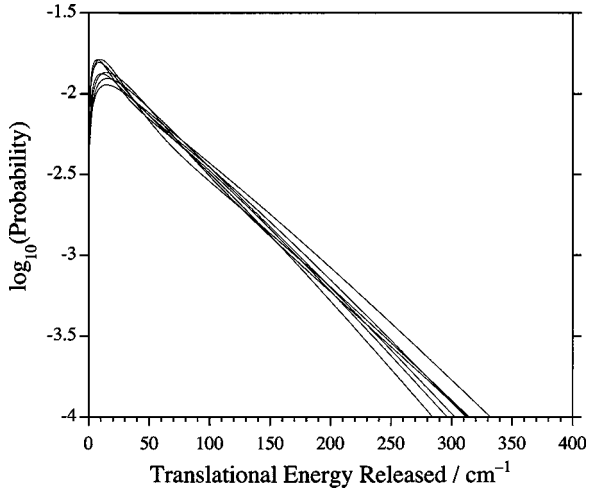

FIG. 4. A plot of the fits to the TER distributions on a logarithmic scale (see Fig. 3 for a plot on a linear scale). The logarithmic plot enhances differences at high energy.

TABLE IV. Values for the average translational energy released during the dissociation of *p*DFB–Ar.

Initial level	Average recoil energy (cm^{-1})
$\overline{5^1}$	60
$\overline{3^1}$	64
$\overline{5^2}$	60
$\overline{3^1 5^1}$	58
$\overline{5^3}$	72
$\overline{3^2}$	62
$\overline{3^2 5^1}$	65

They found average recoil energies for a range of aromatic–Ar complexes to lie in the range $\sim$100–200 cm^{-1}.

The observation that the amount of energy in translation is small can be understood qualitatively using Ewing's momentum gap law that predicts that van der Waals molecule dissociation occurs via channels that minimize the product momentum.[43–45] The theory is based on the overlap of the initial wave function for the van der Waals stretch mode in the vibrationally excited cluster with the wave function describing the momentum of the dissociating fragments. The physical basis for the translational energy minimisation arises from a poor overlap between the translational wave function of the fragments and the initial intermolecular wave function. The rate of predissociation is expressed as[20,44]

$$k_{\mathrm{VP}} \approx 10^{13} \exp[-\pi(\Delta n_v + \Delta n_r + \Delta n_t)], \tag{2}$$

where Δn_v is the change in vibrational quantum number, Δn_r is the change in rotational quantum number, and Δn_t is the change in translational quantum number. Δn_t is given by

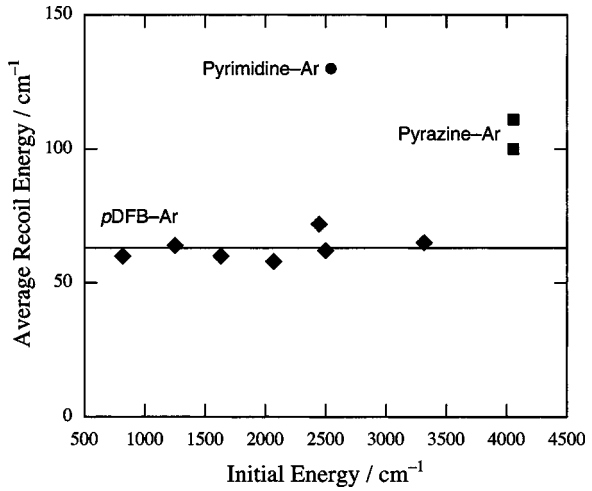

FIG. 5. The average translational energy released in dissociation from each of the initial states of *p*DFB–Ar plotted against the initial vibrational energy (diamonds). The average value is 63 cm^{-1} and is shown by the horizontal line. The energy available to the products is 367 cm^{-1} less than the initial energy. The circle and squares show the average energy transferred to translation in dissociation of the pyrimidine–Ar and pyrazine–Ar complexes, respectively (Ref. 3) (see also footnote to Table I).

$$\Delta n_t = \frac{\sqrt{2\mu\Delta E}}{2a\hbar} - v_z,$$

where μ is the reduced mass of the fragments, ΔE is the final relative translational energy of the fragments, a is the parameter describing the Morse potential for the van der Waals stretch, and v_z is the corresponding vibrational quantum number.

Equation (2) states that dissociation pathways which minimize changes in the vibrational, rotational, and translational quantum numbers have the largest dissociation rate and are preferred. For *p*DFB–Ar, the available experimental observations are in qualitative agreement with this equation. Dispersed fluorescence spectra from initial vibrational levels below $\sim$1000 cm^{-1} show that there is a propensity for product vibrational states with small changes from the initial vibrational quantum numbers of the *p*DFB moiety.[20–23] The translational energy distributions show that there is minimal translational energy released to the products. Our earlier observation that there is significant rotational excitation in the *p*DFB product, at least for dissociation from low vibrational energies, might at first seem anomalous, however, this can also be rationalized as follows.

We have noted previously that anomalous spectroscopic observations can be understood if the *p*DFB–Ar complex accesses bound orbiting states in which the Ar atom is above the barrier to movement from above the plane to below it.[5,27,46] The IVR process that is a precursor to dissociation provides energy to the van der Waals modes, allowing the complex to access bound orbiting states. Calculations show that the barrier to bound orbiting states is well below the dissociation energy.[27] Motion of the Ar atom around the *p*DFB is equivalent to the *p*DFB moiety rotating compared to the Ar atom. In other words, the transfer of energy from the initially excited *p*DFB vibration into the van der Waals modes can lead to rotational motion of the *p*DFB fragment. In such a situation Ewing's model predicts a large proportion of the excess energy following dissociation to be partitioned into the rotational degree of freedom to minimize changes to the rotational quantum number.

The partitioning of energy between product translation and rotation has recently been put on a more quantitative footing with the angular momentum model of McCaffery and co-workers.[47,48] It has been shown that by using an equivalent rotor representation of polyatomics this model can reproduce the total angular momentum in the benzene fragment following dissociation of benzene–Ar.[9] The model also predicts the significant rotational excitation observed in 0° *p*DFB following dissociation of *p*DFB–Ar from $\overline{5^1}$.[9] The success of the calculations points to angular momentum constraints controlling the partitioning of energy between translation and rotation. The angular momentum model calculations predict the rotational distribution for a given final vibrational level; the translational distribution is then determined from the rotational distribution by conservation of energy. Since product vibrational distributions are not known for initial states above 1000 cm^{-1} in *p*DFB–Ar the model cannot be tested against the current data. We also note that with increasing vibrational energy there is a change in the

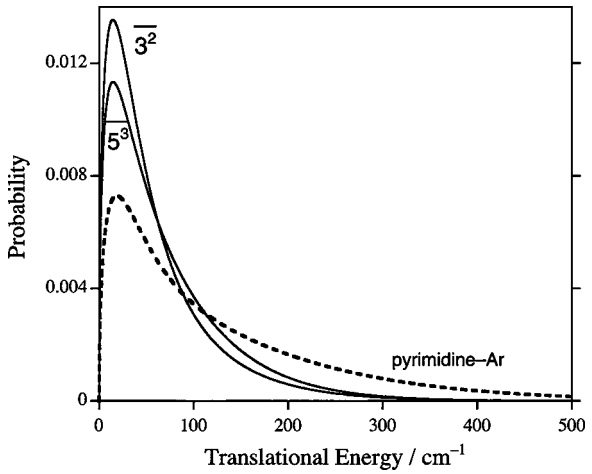

FIG. 6. A comparison of the recoil energy distribution for dissociation of pyrimidine–Ar from within the triplet state (E_{vib}=2589 cm^{-1}) with the *p*DFB–Ar $\overline{5^3}$ (E_{vib}=2447 cm^{-1}) and $\overline{3^2}$ (E_{vib}=2500 cm^{-1}) distributions. The pyrimidine–Ar distribution is shown as the dashed curve.

state-to-state vibrational quantum propensities in low energy collisions involving *p*DFB (Refs. 49 and 50) and, given the potential similarities between van der Waals molecule dissociation and low temperature collision-induced energy transfer,[15] such a change may also occur for the former process. It is clearly desirable to have experimental data concerning product vibrational distributions for dissociation from high lying vibrational levels.

B. Comparison with translational energy release distributions in related systems

There are only two sets of data with which the *p*DFB–Ar results may be compared. The first is Yoder and Barker's study of recoil energies in dissociation from triplet states.[3] Pyrimidine–Ar dissociation was initiated with an initial energy of 2589 cm^{-1}, comparable to that accessed for *p*DFB–Ar. The dissociation energies for the various aromatic–Ar complexes are expected to be similar. The pyrimidine–Ar distribution is compared with the *p*DFB–Ar $\overline{5^3}$ (E_{vib}=2447 cm^{-1}) and $\overline{3^2}$ (E_{vib}=2500 cm^{-1}) distributions in Fig. 6. The pyrimidine–Ar distribution is broader, with more transfer to higher translational energies. The average recoil energy is 130 cm^{-1}, compared with 72 cm^{-1} for $\overline{5^3}$ and 62 cm^{-1} for $\overline{3^2}$. Pyrazine–Ar, at an initial vibrational energy of 4056 cm^{-1}, has a slightly higher initial energy than was probed in our *p*DFB–Ar study. Two experimental distributions were reported, with average recoil energies of 100 and 111 cm^{-1}, again larger than is observed for *p*DFB–Ar. The three T_1 values are included in Fig. 5 for comparison. Transfer to translation is reduced in *p*DFB–Ar compared with the aromatics in Yoder and Barker's study.

The second comparison is with the dissociation of the benzene–Ar cation.[7] In this case there was a distribution of initial energies as the ionisation process produced the cation in a range of vibrational states. The average initial vibrational energy was ~1800–1900 cm^{-1} and the average translational energy released was 92±4 cm^{-1}. Again, this is larger than is observed for *p*DFB–Ar.

The three studies compared involve species in different electronic states, and it is not known whether the electronic state affects TER distributions in van der Waals molecule dissociation. It is known, however, that the electronic state can have a significant effect in the related case of collision-induced energy transfer. Weisman's group has studied collision-induced energy transfer involving pyrazine derivatives in the triplet state.[51–54] They find that the average energy transferred per collision is significantly higher than that for the ground electronic state[55] at the same vibrational excitation. It was proposed that this is due to the lower vibrational frequencies in the triplet state.

C. Insensitivity of the TER distributions to the available energy

That the distributions from the seven levels are so similar is surprising given the range of vibrational state densities covered. The highest level for which the TER distribution has been obtained is $\overline{3^2 5^1}$, which is at a vibrational energy of 3317 cm^{-1}, almost 10× the dissociation energy of 368 cm^{-1}.[4,5] The *p*DFB product can be formed with up to 2949 cm^{-1} in vibration. The density of vibrational states at this energy is 620 per cm^{-1} and there are a total of 2.2 ×10^5 potential destination vibrational levels. Following excitation of $\overline{3^2 5^1}$, IVR will rapidly redistribute the energy into isoenergetic levels and the *p*DFB moiety will have initial excitation in a wide variety of vibrational modes prior to dissociation. Many destination vibrations will be available with low quantum number changes. Nevertheless, dissociation from $\overline{3^2 5^1}$ gives essentially the same translational energy distribution as does dissociation from $\overline{5^1}$, where only two or three *p*DFB product vibrational states are populated[8,20] and *p*DFB is formed with significant rotational excitation.[8] Recently, we have shown that the rotational distribution within the *p*DFB product is consistent with the results of calculations based on the angular momentum model of van der Waals molecule dissociation.[9] This suggests that angular momentum constraints control the partitioning between translation and rotation in dissociation from $\overline{5^1}$. It remains an open question as to whether rotational excitation remains significant as more vibrational states become accessible. Yoder and Barker's calculations suggest that the rotational excitation should decrease, with the average rotational energy becoming similar to the average translational energy.[15] Clearly, data are required concerning the vibrational and rotational energy in the *p*DFB fragments for dissociation at higher energies. It would be remarkable if there were not many more destination vibrations accessed as the vibrational energy increases, especially when rapid IVR occurs within the *p*DFB chromophore prior to dissociation of the complex, yet the distribution of energy in translation appears insensitive to how the energy is partitioned between vibration and rotation in the *p*DFB fragment.

It is interesting in this context to note the "bottleneck" effect seen in collision-induced energy transfer within the triplet state of pyrazine derivatives observed by Weisman's group.[51–54] They find that the average energy transferred per collision increases rapidly with energy above ~2000 cm^{-1}. At lower energies the amount of energy transferred drops to

almost zero. We observe no such change in the translational energy transferred in the half-collision process in *p*DFB.

Yoder and Barker explored whether statistical models could reproduce the TER distributions they observed.[2,3] They found that a statistical model, specifically the "prior distribution," substantially overestimated the energy in translation. Given that the *p*DFB–Ar recoil distributions are narrower than those observed by Yoder, statistical modeling has not been pursued.

D. Supercollisions

An issue of interest is whether the transfer of very large translational energies becomes more probable at higher vibrational energies. Studies of collision-induced energy transfer have found that a small fraction of collisions transfer a large amount of energy, and are referred to as "supercollisions."[56] Calculations show that there is a supercollision like tail in the translational energy distribution for dissociation of pyrazine–Ar and methylpyrazine–Ar van der Waals clusters due to a small proportion of the fragments being ejected with higher translational energies.[15] We do not observe a high energy tail in the *p*DFB distributions. Since the fraction of supercollisions is very small, it is likely that this is because the experiment is not sensitive enough at high energies, where the ions are increasingly spread out and merge with the background. Alternatively, the energies we have investigated may not be large enough to produce a high energy tail in the distribution, although we note that Yoder and Barker did not observe a high energy tail in their recoil energy distributions for complexes with much higher initial energies.

V. CONCLUSIONS

Velocity map imaging has been used to measure the distributions of translational energy released in the dissociation of *p*DFB–Ar van der Waals complexes from vibrational energies in the range 818–3317 cm^{-1}, corresponding to a range of energies above dissociation of 451–2950 cm^{-1}. The translational energy release (recoil energy) distributions are remarkably similar, peaking at very low energy (10–20 cm^{-1}) and decaying in an exponential fashion to approach zero near 300 cm^{-1}. The average translational energy released is small and spans the range 58–72 cm^{-1} for the seven levels studied. The average value is 63 cm^{-1}. The low fraction of transfer to translation is qualitatively in accord with Ewing's momentum gap model.[43–45] No evidence is found in the distributions for a high energy tail, although it is likely that the experiment is not sufficiently sensitive to detect a low fraction of transfer at high translational energies. The average translational energy released is lower than has been seen in comparable systems in different electronic states.

ACKNOWLEDGMENTS

This work was undertaken with the financial support of the Australian Research Council and Flinders University. The authors are grateful for the technical support provided by the staff of the School of Chemistry, Physics, and Earth Sciences Engineering and Electronic Workshops. S.M.B. acknowledges scholarship support from the Australian Government. The authors thank Dr. Jason Gascooke for his contributions to the construction of the velocity map imaging apparatus and the writing of the data analysis software. W.D.L. thanks the Department of Chemistry, University of Canterbury, New Zealand, for their hospitality and the award of an Erskine Fellowship during the writing of this manuscript.

[1] M. F. Vernon, J. M. Lisy, H. S. Kwok, D. J. Krajnovich, A. Tramer, Y. R. Shen, and Y. T. Lee, J. Phys. Chem. **85**, 3327 (1981).
[2] L. M. Yoder, J. R. Barker, K. T. Lorenz, and D. W. Chandler, Chem. Phys. Lett. **302**, 602 (1999).
[3] L. M. Yoder and J. R. Barker, Phys. Chem. Chem. Phys. **2**, 813 (2000).
[4] S. M. Bellm, J. R. Gascooke, and W. D. Lawrance, Chem. Phys. Lett. **330**, 103 (2000).
[5] S. M. Bellm, R. J. Moulds, and W. D. Lawrance, J. Chem. Phys. **115**, 10709 (2001).
[6] R. K. Sampson and W. D. Lawrance, Aust. J. Chem. **56**, 275 (2003).
[7] J. R. Gascooke and W. D. Lawrance, J. Phys. Chem. A **104**, 10328 (2000).
[8] S. M. Bellm and W. D. Lawrance, J. Chem. Phys. **118**, 2581 (2003).
[9] R. K. Sampson, S. M. Bellm, A. J. McCaffery, and W. D. Lawrance, J. Chem. Phys. (in press).
[10] G. Lembach and B. Brutschy, J. Phys. Chem. **100**, 19758 (1996).
[11] G. Lembach and B. Brutschy, J. Phys. Chem. A **102**, 6068 (1998).
[12] D. V. Brumbaugh, J. E. Kenny, and D. H. Levy, J. Chem. Phys. **78**, 3415 (1983).
[13] X. Zang, J. M. Smith, and J. L. Knee, J. Chem. Phys. **97**, 2843 (1992).
[14] H. Saigusa, B. E. Forch, K. T. Chen, and E. C. Lim, Chem. Phys. Lett. **101**, 6 (1983).
[15] L. M. Yoder and J. R. Barker, J. Phys. Chem. A **104**, 10184 (2000).
[16] T. Jayasekharan and C. S. Parmenter, J. Chem. Phys. **120**, 11469 (2004).
[17] P. S. Meenakshi, N. Biswas, G. N. Patwari, and S. Wategaonkar, Chem. Phys. Lett. **369**, 419 (2003).
[18] Z. Q. Zhao and C. S. Parmenter, Ber. Bunsenges. Phys. Chem. **99**, 536 (1995).
[19] D. L. Osborn, J. C. Alfano, N. Vandantzig, and D. H. Levy, J. Chem. Phys. **97**, 2276 (1992).
[20] K. W. Butz, D. L. Catlett, Jr., G. E. Ewing, D. Krajnovich, and C. S. Parmenter, J. Phys. Chem. **90**, 3533 (1986).
[21] H.-K. Oh, C. S. Parmenter, and M.-C. Su, Ber. Bunsenges. Phys. Chem. **92**, 253 (1988).
[22] B. D. Gilbert, C. S. Parmenter, and H.-K. O, J. Phys. Chem. **99**, 2444 (1995).
[23] M.-C. Su, H.-K. Oh, and C. S. Parmenter, Chem. Phys. **156**, 261 (1991).
[24] T. A. Stephenson and S. A. Rice, J. Chem. Phys. **81**, 1083 (1984).
[25] M. R. Nimlos, M. A. Young, E. R. Berstein, and D. F. Kelly, J. Chem. Phys. **96**, 4904 (1992).
[26] M. Becucci, N. M. Lakin, G. Pietraperzia, E. Castellucci, P. Brechignac, B. Coutant, and P. Hermine, J. Chem. Phys. **110**, 9961 (1999).
[27] R. J. Moulds, M. A. Buntine, and W. D. Lawrance, J. Chem. Phys. **121**, 4635 (2004).
[28] H. Koch, B. Fernández, and J. Makarewicz, J. Chem. Phys. **111**, 198 (1999).
[29] B. Fernández, H. Koch, and J. Makarewicz, J. Chem. Phys. **111**, 5922 (1999).
[30] A. E. W. Knight and S. H. Kable, J. Chem. Phys. **89**, 7139 (1988).
[31] R. A. Coveleskie and C. S. Parmenter, J. Mol. Spectrosc. **86**, 86 (1981).
[32] A. T. J. B. Eppink and D. H. Parker, Rev. Sci. Instrum. **68**, 3477 (1997).
[33] L. J. Rogers, M. N. R. Ashfold, Y. Matsumi, M. Kawasaki, and B. J. Whitaker, Chem. Phys. Lett. **258**, 159 (1996).
[34] B.-Y. Chang, R. C. Hoetzlein, J. A. Mueller, J. D. Geiser, and P. L. Houston, Rev. Sci. Instrum. **69**, 1665 (1998).
[35] A. T. J. B. Eppink, S.-M. Wu, and B. J. Whitaker, in *Imaging in Molecular Dynamics*, edited by B. J. Whitaker (Cambridge University Press, Cambridge, 2003), p. 65.
[36] B. A. Jacobson, S. Humphrey, and S. A. Rice, J. Chem. Phys. **89**, 5624 (1988).
[37] E. W. Hanson and P.-L. Law, J. Opt. Soc. Am. A **2**, 510 (1985).
[38] G. Reiser, D. Rieger, T. G. Wright, K. Müller-Dethlefs, and E. W. Schlag, J. Phys. Chem. **97**, 4335 (1993).
[39] R. K. Sampson, S. M. Bellm, J. R. Gascooke, and W. D. Lawrance, Chem. Phys. Lett. **372**, 307 (2003).

[40]N. T. Whetton and W. D. Lawrance, J. Phys. Chem. **93**, 5377 (1989).
[41]W. D. Lawrance and N. T. Whetton, J. Phys. Chem. **93**, 5385 (1989).
[42]X. Zhang, J. Smith, and J. L. Knee, J. Chem. Phys. **100**, 2429 (1994).
[43]G. E. Ewing, Faraday Discuss. Chem. Soc. **73**, 325 (1982).
[44]G. E. Ewing, J. Phys. Chem. **90**, 1790 (1986).
[45]G. E. Ewing, J. Phys. Chem. **91**, 4662 (1987).
[46]R. K. Sampson and W. D. Lawrance, Chem. Phys. Lett. **401**, 440 (2005).
[47]A. J. McCaffery and R. J. Marsh, J. Chem. Phys. **117**, 9275 (2002).
[48]A. J. McCaffery, M. A. Osbourne, R. J. Marsh, W. D. Lawrance, and E. R. Waclawik, J. Chem. Phys. **121**, 169 (2004).
[49]Mudjijono and W. D. Lawrance, Chem. Phys. Lett. **227**, 447 (1994).
[50]Mudjijono and W. D. Lawrance, J. Chem. Phys. **108**, 4877 (1998).
[51]T. J. Bevilacqua and R. B. Weisman, J. Chem. Phys. **98**, 6316 (1993).
[52]D. R. McDowell, F. Wu, and R. B. Weisman, J. Phys. Chem. A **101**, 5218 (1997).
[53]D. R. McDowell, F. Wu, and R. B. Weisman, J. Chem. Phys. **108**, 9404 (1998).
[54]F. Wu and R. B. Weisman, J. Chem. Phys. **110**, 5047 (1999).
[55]L. A. Miller and J. R. Barker, J. Chem. Phys. **105**, 1383 (1996).
[56]U. Hold, T. Lenzer, K. Luther, K. Reihs, and A. Symonds, Ber. Bunsenges. Phys. Chem. **101**, 552 (1997).
[57]L. M. Yoder and J. R. Barker (private communication).